

NA511/96-96-

207114

Reprinted from

NIS

**PROCEEDINGS OF THE
13th WORLD CONGRESS
International Federation of Automatic Control**

San Francisco, USA, 30th June - 5th July 1996

(in 18 volumes)

NAGI-1744

IN-63-CR

©UNIVERSITY

Edited by

Janos J. GERTLER
George Mason University

Jose B. CRUZ Jr
Ohio State University

Michael PESHKIN
Northwestern University

VOLUME H
ROBUST CONTROL II, STOCHASTIC SYSTEMS

Volume Editors

R. BITMEAD (Australia), I. PETERSEN (Australia),
H-F. CHEN (China) and G. PICCI (Italy)

Published for the

INTERNATIONAL FEDERATION OF AUTOMATIC CONTROL

by

PERGAMON

An Imprint of Elsevier Science

—

QFT MULTI-INPUT, MULTI-OUTPUT DESIGN WITH NON-DIAGONAL, NON-SQUARE COMPENSATION MATRICES

R. A. Hess and D. K. Henderson
Dept. of Mechanical and Aeronautical Engineering
University of California
Davis, CA 95616
rahess@ucdavis.edu

ABSTRACT

A technique for obtaining a non-diagonal compensator for the control of a multi-input, multi-output plant is presented. The technique, which uses Quantitative Feedback Theory, provides guaranteed stability and performance robustness in the presence of parametric uncertainty. An example is given involving the lateral-directional control of an uncertain model of a high-performance fighter aircraft in which redundant control effectors are in evidence, i.e. more control effectors than output variables are used.

Keywords: Flight Control, Robust Control, Uncertainty, Decoupling Precompensators

1. INTRODUCTION AND BACKGROUND

A frequent criticism of multi-input, multi-output (MIMO) Quantitative Feedback Theory (QFT) is focused on the use of square plants and diagonal compensation matrices (Yaniv and Horowitz, 1987). The price paid for using such diagonal controllers is in the bandwidth of the resulting design. A number of schemes have been proposed for removing the restriction of diagonal compensation of square plants in MIMO QFT, e.g. (Horowitz, 1991). Most recently, Yaniv (1995) proposed a new approach for obtaining non-diagonal controllers using the so-called "improved" method for QFT design involving sequential loop closures.

In the research to be described, the use of non-diagonal compensators to control non-square plants is demonstrated using the aforementioned sequential QFT design approach. Consider Fig. 1 which shows a MIMO feedback system, with P representing the plant matrix (possibly non-square), and S and G_p representing, respectively, a gain matrix and transfer function matrix both of which are intended to produce an "effective" plant PSG_p which is square and approximately diagonal. The matrix G_c is a square diagonal matrix determined from the QFT design procedure using the square effective plant. As will be seen, the S matrix is a control distribution matrix defined as that which minimizes the weighted sum of the mean square control deflections for a particular P_o in the set Φ (Voulgaris and Valavani, 1991).

The matrix G_p is designed to minimize cross-coupling in the effective plant and uses a methodology first discussed by Catapang, et al (1994).

1.1 Distributing Controls

The control distribution matrix is simply a means for distributing "pseudo-control" outputs to the actual control effectors in any design. Consider the plant dynamics to be given by

$$\begin{aligned} \dot{x}(t) &= Ax(t) + Bu(t) \\ y(t) &= Cx(t) \end{aligned} \quad (1)$$

where

$$\begin{aligned} x &\in R^{nx1} & A &\in R^{nxn} \\ y &\in R^{qx1} & B &\in R^{nxp} \\ u &\in R^{px1} & C &\in R^{qx1} \end{aligned} \quad (2)$$

In the QFT approach one wants the number of pseudo controls to equal the number of outputs, q . Thus, we first define a $B_v \in R^{nxq}$ as any matrix whose column space spans the same column space as B . Write B as

$$B = \begin{bmatrix} B_1 \\ \vdots \end{bmatrix} \quad (3)$$

One immediate choice for B_v is

$$B_v = \begin{bmatrix} I \\ -\dots \end{bmatrix} \quad (4)$$

where I is $q \times q$. The new plant with pseudo-controls is

$$\begin{aligned} \dot{x}(t) &= Ax(t) + B_v v(t) \\ y(t) &= Cx(t) \end{aligned} \quad (5)$$

where $v \in R^{q \times 1}$ and is the pseudo control vector.

Obviously, a transformation between v and u is needed. An optimization procedure can be created to find u so that

$$J = [u^T(t) W u(t)] \quad (6)$$

is minimized, subject to the necessary constraint

$$B_v v - Bu = 0 \quad (7)$$

In Eq. 6, W is a constant diagonal matrix with elements chosen here as the square of the reciprocals of the maximum control effector displacements. Thus, the J in Eq. 6 represents the weighted sum of the instantaneous control effector displacements. The use of Lagrange multipliers shows that the optimal $u(t)$ is given by

$$\begin{aligned} u(t) &= Sv(t) \\ S &= \{W^{-1} B_1 [B_1 W^{-1} B_1^T]^{-1}\} \end{aligned} \quad (8)$$

Of course, plant uncertainty means that the P_0 which is used in determining S will not be optimum for all P in the uncertain plant set ϕ . However, this is a small price to pay for a very simple technique for producing a square plant and is superior to the somewhat *ad hoc* techniques which have been previously proposed (Hamilton, et al, 1989). In addition, it can be shown that S can be changed, i.e. the weighting matrix used in the optimization procedure can be altered, with *no* change required in the compensation G_c or G_p in Fig. 1 (Voulgaris, and Valavani). This means, for example, that if there exists control redundancy,

i.e. more control effectors that outputs being controlled, a very simple approach to control reconfiguration is possible in the event of failure of one of the control effectors. Essentially one precomputes a number of S matrices, say S_i , $i = 1, \dots, n_s$, where n_s is the number of control effectors. Each S_i is calculated with the weighting element on δ_i to infinity. Assuming that the inoperative or damaged control effector can be identified, the S matrix in Fig. 1 can be replaced by S_k (δ_k being the inoperative/damaged control effector) and the control load distributed to the remaining effectors, with no change in G_c or G_p . The stability and performance characteristics of the resulting system will be identical to those of the original system.

1.2 Minimizing Control Cross-coupling

The matrix of transfer functions G_p is designed to reduce the control cross-coupling in the square, modified plant PS . Taking a 2×2 modified plant as an example,

$$PS = \begin{bmatrix} P_{m_{11}} & P_{m_{12}} \\ P_{m_{21}} & P_{m_{22}} \end{bmatrix} \quad (9)$$

Then G_p takes the form

$$G_p = \begin{bmatrix} 1 & G_{p_1} \\ G_{p_2} & 1 \end{bmatrix} \quad (10)$$

Now, in the absence of uncertainty, one could write

$$G_{p_1} = -\frac{P_{m_{12}}}{P_{m_{11}}} \quad G_{p_2} = -\frac{P_{m_{21}}}{P_{m_{22}}} \quad (11)$$

and exact decoupling would occur. However in the presence of uncertainty, one must choose G_{p_1} and G_{p_2} so that (1) Eq. 11 is approximately satisfied over ϕ , and (2) the resulting G_{p_1} , G_{p_2} are stable and proper. This task is best accomplished by transfer function fits in the complex plane. Space does not permit a discussion here.

1.3 The Final Compensator

The final compensator, i.e. the one which is implemented in the control system of Fig. 1, is

$$G = SG_p G_c \quad (12)$$

where $G \in \mathbb{R}^{p \times q}$

2. DESIGN EXAMPLE

To exemplify the proposed methodology, an aircraft flight control problem was chosen. The task and vehicle are the lateral-directional control of a supermaneuverable fighter aircraft based upon the F-18 and shown in Fig. 2. The response variables were roll-rate about the velocity vector, p , and sideslip, β . Five control effectors were used. These were δ_{DT} , differential horizontal stabilizer, δ_A , aileron, δ_R , rudder, δ_{RTV} , differential pitch thrust vectoring, and δ_{YTV} , yaw thrust vectoring. The vehicle dynamic model was taken from Adams, et al (1992). Plant uncertainty resulted from considering 15 different equilibrium flight conditions defined by altitude and Mach No. The altitude varied from 10,000 to 30,000 ft, and Mach No. varied from 0.3 to 0.9, depending upon altitude.

The control distribution matrix S was found by using a weighting matrix based upon the square of the reciprocals of the maximum control effector deflections for a nominal plant case. The matrix G_p was chosen to reduce control cross-coupling in the modified plant PS for all P in the plant set Φ . Tracking bounds were selected based upon estimates of acceptable performance. Cross-coupling bounds were selected as follows: First, the compensation elements in G_c were approximated around their crossover frequencies as

$$G_{c_p} \approx \frac{\omega_{c_p}}{s} \frac{1}{(PSG_p)_{pp}} \quad (13)$$

$$G_{c_\beta} \approx \frac{\omega_{c_\beta}}{s} \frac{1}{(PSG_p)_{\beta\beta}}$$

where

$$(PSG_p)_{pp} \text{ and } (PSG_p)_{\beta\beta}$$

represent the diagonal elements of the effective plant transfer function matrix PSG_p . The crossover frequencies ω_{c_p} and

ω_{c_β} were then varied until the performance bounds could be met across all the plants. Second, greatest upper bounds on the magnitudes of the transfer functions β/p_c and p/β_c which were then in evidence were used as the cross-coupling bounds in the QFT design.

Figures 3-6 show the resulting system performance in tracking and cross-coupling responses. Table 1 lists the compensators, prefilters and the crossover frequencies, the latter for the nominal plant. The sequential design began with the β loop. It should be noted that, without inclusion of the G_p matrix, the design could not be completed with reasonable loop bandwidths. As the figures show, excellent performance was obtainable with the design procedure, despite the fact that significant uncertainty existed in P and that considerable cross-coupling was evident between roll-rate and sideslip in the basic airframe.

3. CONCLUSIONS

A technique for the QFT design of MIMO systems using non-diagonal, non-square compensation matrices has been formulated and exercised on a challenging flight control problem. The technique does not rely upon *ad hoc* design procedures for producing an effective plant which is square and approximately non-diagonal. Ongoing research is aimed at determining better techniques for choosing the control distribution matrix and for accommodating the effects of possible actuator saturation.

REFERENCES

- Adams, R. J., Buffington, J. M., Sparks, A. G., and Banda, S. S., 1992, "An Introduction to Multivariable Flight Control System Design, WL-TR-92-3110, WPAFB, OH.
- Catapang, D. R., Tischler, M. B., and Biezad, D. J., 1994, "Robust Crossfeed Design for Hovering Rotorcraft," *International Journal of Robust and Nonlinear Control*, Vol. 4. No. 1, pp. 161-180.

Hamilton, S. Horowitz, I., and Houppis, C. H., 1989, "QFT Digital Controller for an Unmanned Research Vehicle (URV)", American Control Conference, pp. 2441-2452.

Horowitz, I., 1991, "Survey of Quantitative Feedback Theory (QFT)," *International Journal of Control*, Vol. 53, No. 2, pp. 255-291.

Voulgaris, P., and Valavani, L., 1991, "High Performance Linear-Quadratic and H-Infinity Designs for a "Supermaneuverable" Aircraft," *Journal of Guidance, Navigation and Control*, Vol. 14, No. 1, pp. 157-165.

Yaniv, O., and Horowitz, I., 1987, "Quantitative Feedback Theory - Reply to Criticisms," *International Journal of Control*, Vol. 45, No. 3, pp. 945-962.

Yaniv, O., 1995, "MIMO QFT Using Non-Diagonal Controllers," *International Journal of Control*, Vol. 61, No. 1, pp. 245-253.

Table 1 QFT Design Results

Compensators:^a

$$G_{c_p} = \frac{7.15 \cdot 10^5 (0.16)(2.95)[1, 11.8](48)}{(0)(400)^3 [0.76, 2.15]}$$

$$G_{c_p} = \frac{2.6 \cdot 10^5 [0.12, 1.48][0.12, 2][1, 0.53][0.89, 45]}{(0)(125)(300)^3 [0.49, 0.9][0.078, 2.36]}$$

$$^a \frac{K(z_1)}{(p_1)[\zeta_{p_1}, \omega_{p_1}]} = \frac{K(s+z_1)}{(s+p_1)[s^2+2\zeta_{p_1}\omega_{p_1}s+\omega_{p_1}^2]}$$

Prefilters:

$$F_p = \frac{288.5(1.98)(2)}{(2.3)^2(12)(18)}$$

$$F_p = \frac{500(0.8)}{(1)(2)(4)(50)}$$

Nominal Crossover Frequencies:

$$\omega_{c_p} = 7 \text{ rad/s} \quad \omega_{c_p} = 5 \text{ rad/s}$$

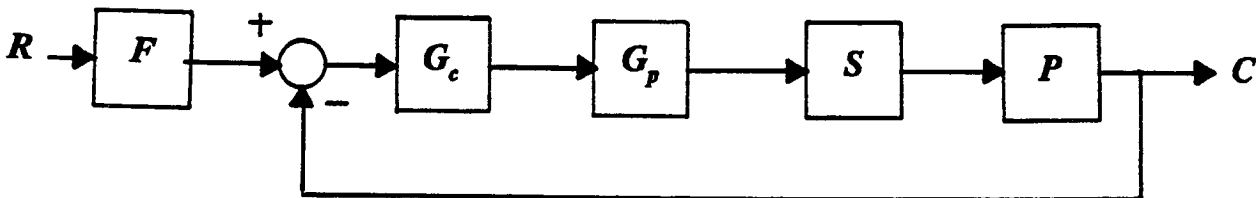


Figure 1: A MIMO feedback system

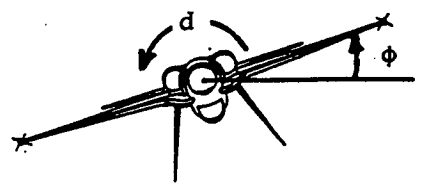
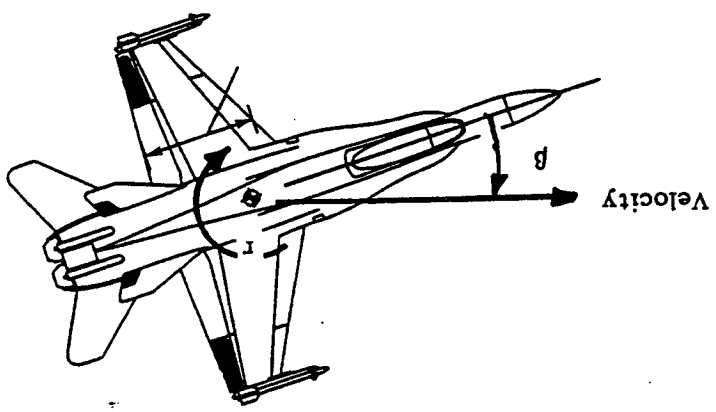


Figure 2: The supermaneuverable fighter

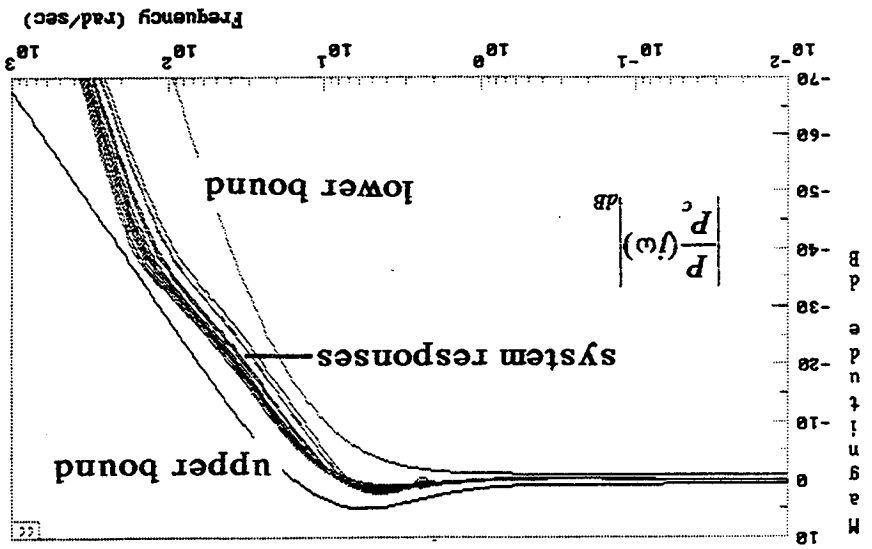


Figure 3: Roll-rate tracking responses in QFT design

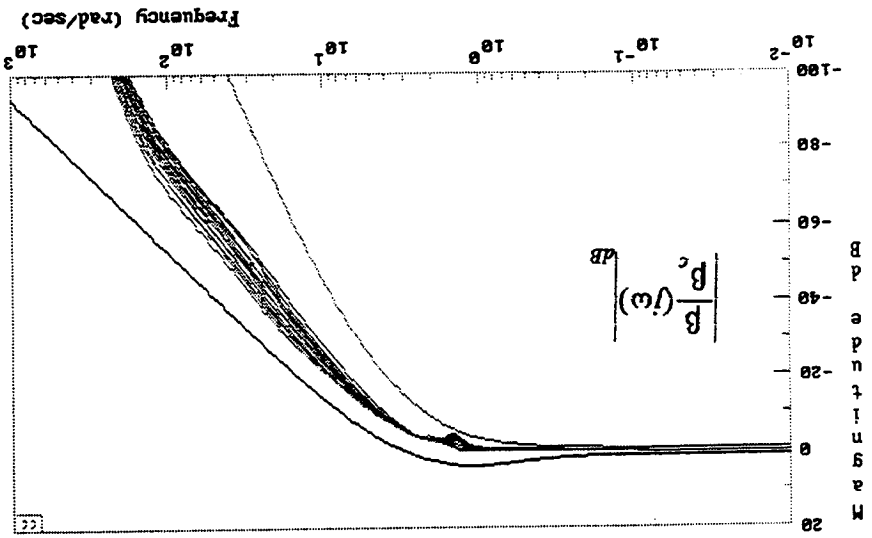


Figure 4: Sideslip tracking responses in QFT design

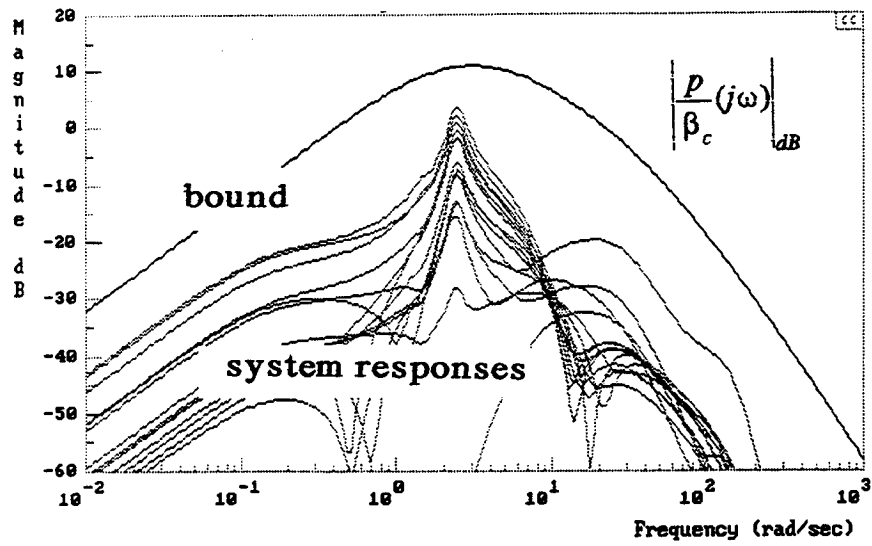


Figure 5: Roll-rate to sideslip command responses in QFT design

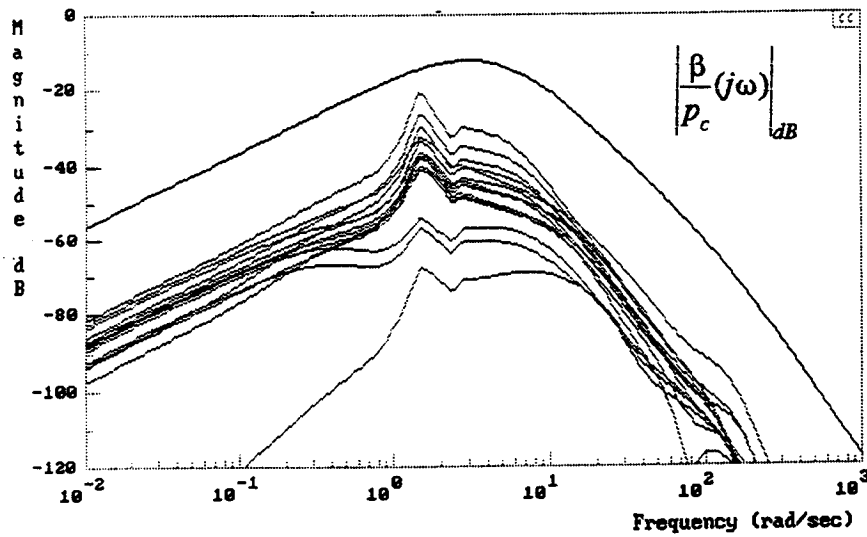


Figure 6: Sideslip to roll-rate command responses in QFT design